



## THE DETERMINATION OF THE HEAT EXTRACTION RATIO IN THE SOLAR POND

Hacı SOGUKPINAR\* and Ismail BOZKURT\*\*

\* Department of Electric and Energy, Vocational School, University of Adiyaman, Adiyaman 02040, Turkey, [hsogukpinar@adiyaman.edu.tr](mailto:hsogukpinar@adiyaman.edu.tr), ORCID: 0000-0002-9467-2005

\*\*Department of Mechanical Engineering, Faculty of Engineering, University of Adiyaman, Adiyaman 02040, Turkey, corresponding author, [ibozkurt@adiyaman.edu.tr](mailto:ibozkurt@adiyaman.edu.tr), ORCID: 0000-0002-2126-3710

(Geliş Tarihi: 09.06.2021, Kabul Tarihi: 26.11.2021)

**Abstract:** In this study heat extraction ratio of a solar pond was investigated numerically by using the Discrete Ordinates Method (DOM) with the direct solver PARDISO by using nested dissection multithreaded preordering algorithm, and the findings without exchanger were compared with experimental data to validate simulation accuracy of numerical approaches in the Mediterranean climatic condition. The solar pond was modeled with the same dimension as a previous experimental system and a heat exchanger was placed in the heat storage zone and simulation to take out the hot water at a certain flow was performed with the commercial software COMSOL. The solar position was defined for Adana and ambient data was obtained by processing the ASHRAE Weather Data Viewer 5.0. As a result, the maximum and minimum heat extraction ratio (HER) is calculated as 13.39 % in July and 2.96 % in September for a flow rate of 0.007 kg/s; 24.27 % in June, and 3.23 % in September for a flow rate of 0.014 kg/s, respectively.

**Keywords:** Solar energy, solar pond, thermal energy, heat transfer, heat exchanger

### GÜNEŞ HAVUZLARINDA ISI ÇEKME ORANININ BELİRLENMESİ

**Özet:** Bu çalışmada, bir güneş havuzunda ısı çekme oranı, doğrudan çözücü PARDISO ile Ayrık Ordinatlarda Yöntemi kullanılarak iç içe parçalara ayrılıp çok iş parçacıklı ön düzenleme algoritması ile sayısal olarak araştırılmış ve sayısal yaklaşımların simülasyon doğruluğu için eşanjörsüz güneş havuzunda yapılan ön nümerik sonuçlar deneysel verilerle Akdeniz iklim koşullarında karşılaştırılmıştır. Daha sonra, güneş havuzu önceki bir deney sistemi ile aynı boyutta modellenmiş ve ısı depolama bölgesine bir ısı eşanjörü yerleştirilmiş ve COMSOL ticari yazılımı ile sıcak suyun belirli bir akışta dışarı alınması için simülasyon gerçekleştirilmiştir. Adana için güneş konumu tanımlanmış ve ASHRAE Weather Data Viewer 5.0 ile işlenerek ortam verileri elde edilmiştir. Sonuç olarak, 0.007 kg/s debi için maksimum ve minimum ısı çekme oranı Temmuz ayında % 13.39 ve Eylül ayında % 2.96 olarak hesaplanmıştır; 0.014 kg/s debi için sırasıyla Haziran'da %24.27 ve Eylül'de %3.23'tür.

**Anahtar kelimeler:** Güneş enerjisi, güneş havuzu, ısı enerjisi, ısı transferi, ısı eşanjörü

#### NOMENCLATURE

E	Energy (J)
exc.	Exchanger
C <sub>p</sub>	Specific heat capacity at constant pressure (J/kg°C)
h	Heat transfer coefficient (W/m <sup>2</sup> K)
DOM	Discrete Ordinate Method
HSZ	Heat storage zone
I (Ω)	Radiative intensity at a given position following the Ω direction
I <sub>b</sub> (T)	Blackbody radiative intensity
I(Ω)	Radiation density in a place in Ω direction
k	Thermal conductivity (W/m K)
NCZ	Non-convective zone
N <sub>r</sub>	Refractive index
n	Outward normal vector

p	Pressure (Pa)
S	Strain-rate tensor (1/s)
T	temperature (K)
Q	Heat sources other than viscous heating (W/m <sup>3</sup> )
q <sub>r</sub>	Heat flux striking the wall
q	Heat flux by conduction (W/m <sup>2</sup> )
UCZ	Upper convective zone
u	Velocity vector (m/s)
U	Internal energy (J)

#### Greek symbols

κ	absorption coefficients
β	extinction coefficients
σ <sub>s</sub>	Scattering coefficients
φ	Scattering phase function
τ	Cauchy stress tensor deviator

$\sigma$	Stefan-Boltzmann constant
$\rho$	Density (kg/m <sup>3</sup> )

#### Subscripts

exch	exchanged
ext	extracted
st	stored
sw	side wall

## INTRODUCTION

The effects of global warming on the environment have started to emerge as different natural disasters all over the world. Therefore, many countries have made very comprehensive investments in alternative renewable energy sources. On the other hand, global energy costs are quite high and foreign energy-dependent countries economy has been shaken. Due to both economic and environmental factors, it has become a necessity for countries to generate their energy from their own resources. The only renewable energy source that countries can harness equally is solar energy all over the world. Solar energy thermal systems are one of the technologies which have advanced and are widely used for many industrial processes such as heating, cooling, product drying, providing low-grade hot water, water desalination, direct steam provision, and commercial cooking (Renewables 2017 Global Status Report, 2018). Solar ponds are thermal energy systems that convert solar energy into heat and have the capacity to store it for a long time. Solar ponds have many operational advantages, such as: easier to construct and set up, lower maintenance rate and installation cost, and long-term energy storage potential. Many studies have been carried out on the heat energy storage capacity of solar ponds. Bozkurt et al. (2012) studied the efficiency of the solar pond which was integrated with flat plate collectors. The efficiency increase of the integrated system was investigated. The energy and exergy analysis of an experimental solar pond, coupled with solar collectors were calculated and compared by Karakilcik et al. (2013a). Furthermore, Karakilcik et al. (2013b) investigated the shading effect on model solar ponds. The efficiency of the solar ponds with and without shading effect was investigated and the shading coefficients of the model pond were determined. The effect of transparent covers on the performance of the solar pond was investigated in another study by Bozkurt et al. (2014), separately. The energy efficiency of the solar pond was calculated for each cover, and the glass cover was determined as the best for the solar ponds. On the other hand, Bozkurt et al. (2015) have determined the effects of a parameter on the thermal performance of sunshine area rates of a model solar pond of different sizes. The performance of solar ponds was also investigated by Sogukpinar et al. (2016; 2018) for different conditions. The annual seasonal temperature distributions of the solar pond were investigated and the efficiency of the system was

calculated. For the salt-gradient solar pond, heat extraction and its variation were investigated by Alcaraz et al. (2016). The pond was tested and compared to conventional heat exchangers for the sidewall areas. The effect of phase change materials on the efficiency of the pond was investigated experimentally by Assari et al. (2015). In order to improve the thermal energy storage capacity of the solar pond, two models were built with and without phase change material to determine its stability during heat extraction. The performance of NCZ and HSZ was investigated to determine the efficiency of the solar pond by Date et al. (2013). For this, a simple method was proposed to estimate the transient thermal performance of the system when heat is extracted from different parts of the pond. The activity of the shallow solar pond under open and closed cycle modes was studied both experimentally and numerically by El-Sebaï et al. (2013) and heat extraction was optimized and compared to show the availability of solar pond in domestic heating and industrial usage. The effect of heat extraction in the non-convective region on the performance of an experimental solar pond was shown by Leblanc et al. (2011) and the performance of the solar ponds was improved by the conventional heat extraction method. Aramesh et al. (2017) investigated the heat storage and heat extraction processes of solar ponds with a combination of the methods presented in the previous works, theoretically. The impacts of different nano-fluids on the heat extraction operation of solar ponds were studied. Khalilian et al. (2018) developed different heat extraction models to determine the effects on the efficiency of the solar pond. The energetic and exergetic transient performances were compared under different modes of heat extraction. Mansouri et al. (2018) suggested three different heat extraction technics to evaluate the performance of the solar pond. The technics were compared based on outlet temperatures and amounts of energy and exergy extraction. Amirifard et al. (2018) compared temperature changes and thermal energy to determine the latent heat storage in the solar ponds for performance stability without phase change material. The heat extraction from the solar pond and the heat supply processes was evaluated by Alcaraz et al. (2018). The heat extraction and supply tests were carried out for a conventional and lateral wall heat exchanger.

Generally, high concentrated brine has been used in solar ponds. Therefore, heat energy from the system cannot be harnessed directly but exchanger. Therefore, the heat storage efficiency of the solar pond alone has no meaning but integrated with a heat exchanger it expresses something for efficiency. Furthermore, when the heat is extracted, the real behavior of the pond emerges. Thus, the ratio of the energy stored in the pond to the energy coming to the pond surface can be

increased. On the other hand, there is a lot of investigation, are available related to the efficiency of the solar pond with a simple analytic method but it is rare with a comprehensive method like Discrete Ordinate Method (DOM). Therefore in this study, the performance of solar pond with an exchanger under Mediterranean climatic conditions was investigated for the full year of operations by using discrete ordinates method and compared with experimental data to validate numerical approaches. The outflow water temperature of a heat exchanger was calculated for the inflow rate temperature of 20°C and the heat extraction ratio of the system was calculated and discussed.

## METHODOLOGY

### Heat transfer mechanism

The radiation can interact with the surface or the environment in different ways such as absorption, emissions, scattering, and transmission. Interacted medium absorbs a part of the incident radiation and a fraction of radiation is emitted and scattered in all directions, and a part of it may be transmitted to another medium. Heat energy, transmitted from one medium to another via conduction, convection, and thermal radiation, depending on the state of the systems. Heat conduction happens oscillations of each molecule in fluids, in metals mainly by heat-carrying electrons but in gas which occurs through collisions of molecules. Convection occurs with a net displacement of a heat-transferring fluid. Balance of radiative transfer between source and interacting medium happens. The general radiative transfer equation can be written with Eq.(1) (COMSOL, 2018; Modest, 2013).

$$\Omega \cdot \nabla I(\Omega) = \kappa I_b(T) - \beta I(\Omega) + \frac{\sigma_s}{4\pi} \int_{4\pi} I(\Omega') \varphi(\Omega', \Omega) d\Omega' \quad (1)$$

Where,  $I(\Omega)$  represent the radiative intensity in a given ( $\Omega$ ) direction,  $I_b$  is the blackbody radiation intensity,  $\kappa$ ,  $\beta$ ,  $\sigma_s$  are absorption, extinction, and scattering coefficients. Radiative intensity may be defined for any direction  $\Omega$  due to continuous properties of angular space. This discrete ordinates method is used to approximately solve approximately the radiation transfer equation by discretizing both the xyz-domain and the angular variables that specify the direction of radiation. This method provides a discretization of angular space into  $n = N(N + 2)$  in 3D discrete directions. The following Eq.(2) was used for the discretization in 3D (COMSOL, 2018).

$$S_i \cdot \nabla I_i = \kappa I_b(T) - \beta I_i + \frac{\sigma_s}{4\pi} \sum_{j=1}^n w_j I_j \Phi(S_i, S_j) \quad (2)$$

where,  $S_i$  is the  $i^{\text{th}}$  discrete ordinate,  $w_j$ , is weight. Rosseland and P1 approximation are another possible radiation discretization method. In this study, DOM was used. Because Rosseland approximation has a

limited impact from a computational point of view and does not provide any extra degree of freedom to the heat equation and P1 approximation provides only one additional degree of freedom. For the current simulation, refractive index ( $n_r$ ) was taken as 1, the index set to 0.4. The radiation with participating media interactions was calculated by using Eq.(2). Heat transfer in solid and liquid and was calculated by using the following Eq.(3) (COMSOL, 2018).

$$\rho C_p \left( \frac{\partial T}{\partial t} + \rho C_p \mathbf{u} \cdot \nabla T \right) + \nabla \cdot \mathbf{q} = Q + Q_{ted} + Q_r \quad (3)$$

where  $\mathbf{q} = -\mathbf{k}\nabla T$ ,  $Q_r = \kappa(\sum_{i=1}^N w_i I_i - 4\pi I_b)$ ,  $Q_r$  is used to calculate heat flux divergence in the participating media.  $\mathbf{k}$  is thermal conductivity,  $\rho$  is the density of medium which can be solid, liquid and gas depend on the boundary region.  $C_p$  is the heat capacity,  $T$  is temperature,  $\mathbf{q}$  is the heat flux,  $Q$  is heat, and  $Q_{ted}$  is the thermoelastic damping heat source. Eq.(3) is used to calculate heat transfer and the same equation is used for the liquid but  $Q_{ted}$  is replaced by  $Q_p + Q_{vd}$ .  $Q_p$  is work done under pressure,  $Q_{vd}$  represents viscous dissipation in the fluid. Heat transfer module was used to calculate heat transfer with radiation in participating media and heat transfer in solid and liquid. For this Eq.(2) and Eq.(3) were used to calculate radiation in participation media, Eq.(2) was used to calculate heat transfer in liquid and solid. Eq.(3) was used for calculation of heat interaction with exchanger.

### Boundary conditions

Meteorological data was defined for the experiment period from 2011 to 2012 for Adana. The initial condition was set as average wind speed and temperature. The physical properties of materials were taken from COMSOL library. For the heat flux from the surface to air, convection was defined and meteorological data was defined for outside conditions. For the fluid inside the pipe and heat exchanger, fluid velocity was set from 0-2 cm/s, heat conductivity, the ratio of specific heat, and heat capacity from liquid to solid and solid to liquid was defined from used materials automatically. The inflow velocity of water into the heat exchanger was defined as 293.15 K and the other end of the pipe was defined as outflow. The general layout of the solar pond coupled with the exchanger is as shown in Figure 1. Since the solar pond is semitransparent, a part of the incoming solar ray is reflected and scattered and some of it is absorbed by the saltwater and turned into heat. Part of the stored heat is escaped around the environment by conduction, convection, and radiation.

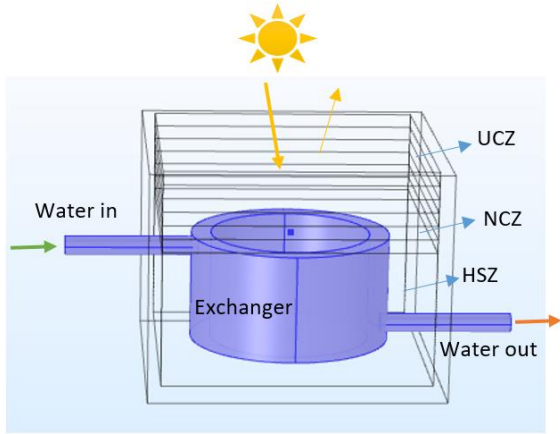


**Figure 1.** The general layout of the heat exchanger in the solar pond

The Heat Storage Zone (HSZ) is 1 m deep, the Non-Convective Zone (NCZ) consists of 4 layers each has a depth of 0.10 m, and Upper Convective Zone (UCZ) has one layer with 0.10 m deep. The pond was insulated with foam with the thickness of 0.10 m and also inlet and outlet pipes were insulated with 0.05 m thick foam due to their physical size. The NCZ undertakes upstream insulation of the heat storage zone, so with the increasing number of layers at a certain level, which increases the thermal insulation. A shell-type exchanger, with a thickness of 0.15 m and a depth of 0.80 m was designed with inlet and outlet pipes diameter of 0.03 m, and was integrated into the system.

### Geometry and Mesh generation

The mesh module in COMSOL was used to create the mesh. Figure 2 shows the mesh distribution in the solar pond. Too sparse mesh distribution may produce calculation error but too dense distribution increase computational time. It was observed that the high mesh distribution greatly increased the computation time but there was no difference compared to the lower mesh distribution. For the numerical calculation in the literature, the only criteria are general compliance with the experiment. Therefore, only the results are more agreement with the experiment were used. 39,693 tetrahedral mesh elements were created. In order to make a more accurate calculation, the mesh distribution in the inlet and outlet sections of the pipe was increased. The mesh quality was determined 0.68 and the minimum was 0.23. Direct solver PARDISO was used for the simulation. Iteration technics and nonlinear methods were used for termination and method. Two other direct solvers in COMSOL are available such as MUMPS and SPOOLES. On the other hand, PARDISO is fast, robust, multi-core capable, and scales better than MUMPS on a single node with many cores but SPOOLES is slow (COMSOL, 2018).

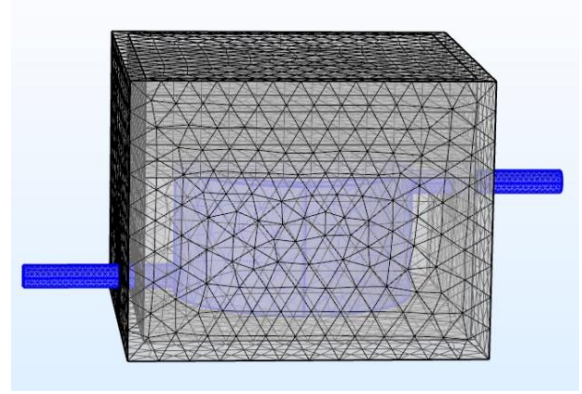


**Figure 2.** Mesh distribution of the solar pond

### Heat Extraction ratio

The heat energy extraction from solar ponds is very important in terms of the efficiency of the pond and heat extraction keeps the temperature in the solar pond at a certain level. Therefore, the heat losses would be reduced. On the other hand, the extracted heat can be used in for various purposes. Solar ponds store the solar energy, coming to the surface of the pond, as heat in the storage zone. The heat is extracted from the solar pond by the heat exchanger in the form of a cylindrical shell, placed in HSZ. The ratio of the extracted heat to incoming solar energy (heat extraction ratio, HER) is calculated as follows.

$$HER = \frac{Q_{ext.}}{Q_{solar}} \quad (4)$$

where  $Q_{ext.}$  is the monthly total heat extracted from the solar pond,  $Q_{solar}$  is the monthly total solar energy incoming to the surface of the solar pond. The monthly total heat extraction was calculated as;

$$Q_{ext.} = \sum_{\Delta t} \dot{m} c_p (T_{out} - T_{in}) (\Delta t) \quad (5)$$

### RESULTS AND DISCUSSIONS

The numerical calculation was conducted by using discrete ordinates method (DOM) and compared with experimental data to validate the simulation accuracy of the numerical approaches. For solar energy and ambient data ASHRAE, Weather Data Viewer 5.0 was used starting from 2010. It is the construction time of the experimental system. The experimental system was built in 2005 and the performance of a solar pond was investigated (Karakilcik et al., 2006), which was integrated with solar collectors (Bozkurt et al., 2012), dynamic exergetic performance assessment of an integrated solar pond (Karakilcik et al., 2013a) was observed, solar pond with and without shading effect (Karakilcik et al., 2013b) was investigated, transparent covers on the performance (Bozkurt et al., 2014), and effect of sunny area ratios on the thermal performance of solar ponds (Bozkurt et al., 2015) and related some

parameter has been investigated and reported since then. On the other hand, varied analytic methods have been used for numerical calculation in addition to experiments but no comprehensive method like DOM has been used. Figure 3 shows yearly solar radiation and ambient temperature distributions for Adana, in Turkey.

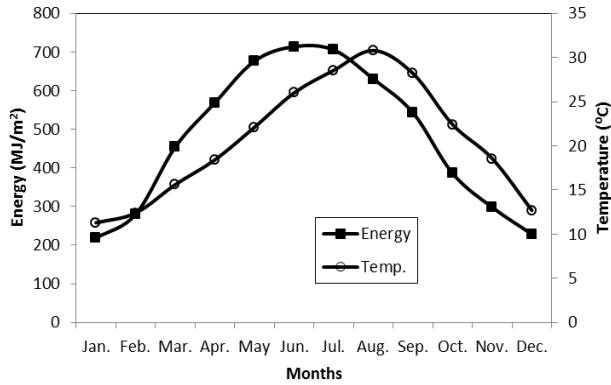


**Figure 3.** The solar energy and ambient temperature distributions for Adana, Turkey, 2010 (Adana Meteorology Regional Office, 2018) Maximum and minimum incident solar energy on the surface of the solar pond is 713.91 MJ/m<sup>2</sup> in June and 218.48 MJ/m<sup>2</sup> in January, and the monthly average maximum and minimum temperatures are observed 30.80 °C in August and 11.30 °C in January, respectively.

The temperature was measured by a sensor for each 0.10 m from the test set and for the numerical model, the temperature was calculated instantaneously at 0.10 m, 0.50 m, and 0.90 m from the base and is presented in Figure 4b. The numerical calculation was carried out for 14 months to see seasonal variation temperature, starting from the first day of March, and is given in Figure 4 with the experimental measurement (Karakilcik et al., 2006). Numerical calculations were carried out in succession for every 30 days and the temperature distribution of the system for May is given in Figure 4a. The numerical study for the whole year is given in Figure 4.b as a line graph in comparison with the experimental study.

There is almost a good agreement between the theoretical data and the experiment. Numerical study results are given for 10, 50, and 90 cm depths of the heat storage zone, and although there are small deviations in winter, they are generally in full agreement. In order to achieve this compliance, meteorological data of the experiment time were defined exactly to the numerical method.

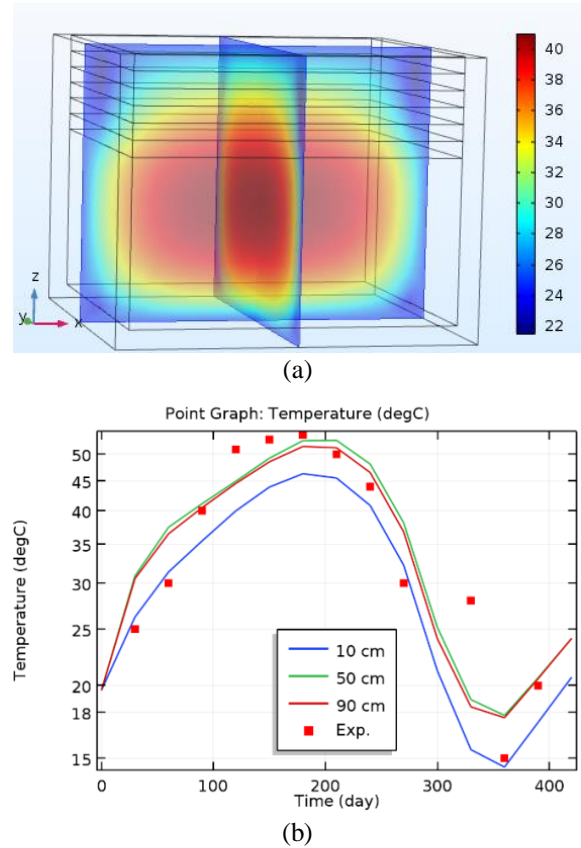


**Figure 4.** The temperature distribution in the pond without exchanger; (a) temperature distribution (b) temperature point graph for different depths

In preliminary calculations, when the calculation started from January, the calculated solar pond temperature was quite low and bumpy until the end of February. Therefore, to ensure temperature compatibility between experiment and theory, the calculation was started from the first day of March and the numerical method was conducted for 14 months to observe seasonal temperature distribution.

The performance of the solar pond with a heat exchanger was tested by increasing the water flow rate to 0.007 kg/s (1 cm/s) and 0.014 kg/s (2 cm/s). The temperature distribution in different depths of the solar pond for different flow rates is given in Figure 5. It is seen that more heat can be extracted from the system with an increasing flow rate. The maximum water temperature taken out at a speed of 1 cm/s is 42 °C, while the maximum water temperature at a speed of 2 cm/s is around 37 °C. This shows heat can be drawn from the solar pond in summer and spring with the help of an exchanger. however, it was determined that extra heating is not possible at an inlet temperature of 20 °C in winter periods. Fig. 6 shows the outflow temperature distribution of the heat exchanger.

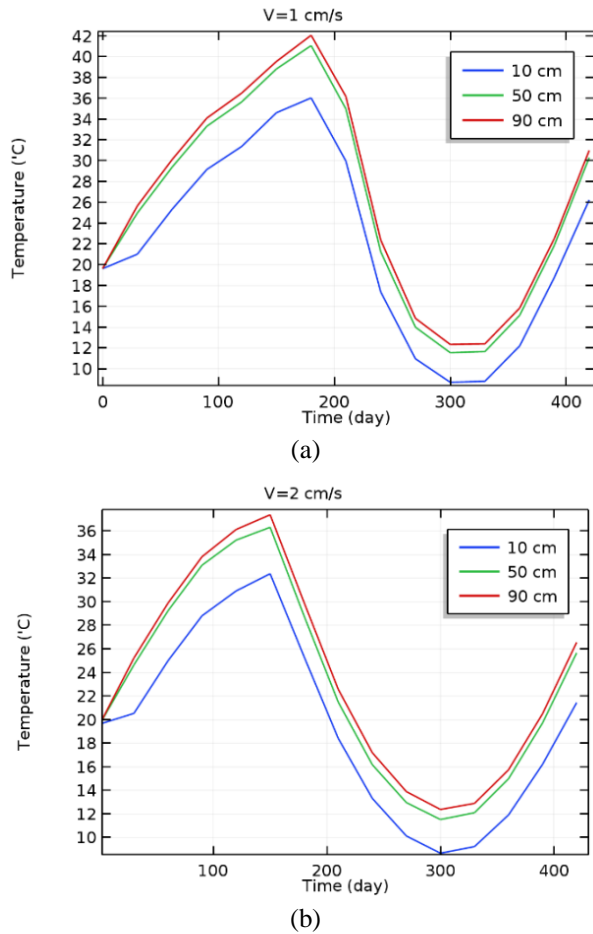


**Figure 5.** Seasonal temperature variations in different depths of solar pond for different flow rates (a) 1 cm/s (0.007 kg/s) (b) 2 cm/s (0.014 kg/s)

The outflow temperature of the exchanger from March to September is calculated higher than inlet temperature ( $20\text{ }^{\circ}\text{C}$ ) and is calculated lower than the inlet temperature from October to February. Solar ponds can be used for primary heating in winter and some of the autumn months then the inlet temperature ( $0\text{ }^{\circ}\text{C}$  to  $20\text{ }^{\circ}\text{C}$ ) might be increased a few degrees up to a maximum  $20\text{ }^{\circ}\text{C}$ . Then the temperature could be raised to the desired point by using a hybrid system.

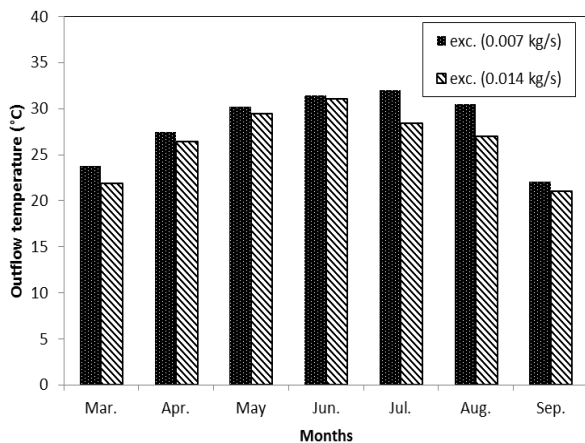


**Figure 6.** The monthly average outflow temperature of the heat exchanger

Heat loss is one of the most important factors, affecting the performance of the system. The heat losses from the solar pond were calculated separately for the case where the heat was extracted not extracted. Fig.7 shows the heat losses from the solar pond with and without an exchanger. The heat losses reach maximum at the time when the temperature difference between the solar pond and ambient temperatures is maximum. On the other hand, heat losses are reduced by extracting heat from the solar pond.

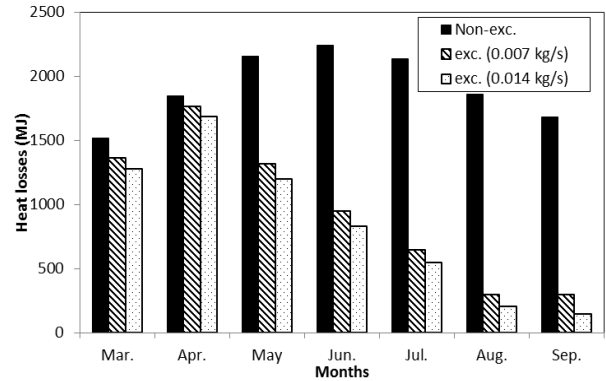


**Figure 7.** Total heat losses from the solar pond for with and without heat exchanger

The heat was extracted from the solar pond with the cylindrical shell heat exchanger in the heat storage zone of the solar pond. The inlet temperature of the heat exchanger was determined as  $20\text{ }^{\circ}\text{C}$ , the output temperatures of the heat exchangers were measured for different flow rates. The equation is given in Eq. 5, and the amount of extracted heat from the solar pond was calculated monthly. Figure 8 shows the extracted heat from the solar pond for different flow rates. The maximum and minimum extracted heats are  $377.63\text{ MJ}$  in July and  $64.29\text{ MJ}$  in September for the flow rate  $0.007\text{ kg/s}$ ;  $692.99\text{ MJ}$  in June and  $70.13\text{ MJ}$  in September for  $0.014\text{ kg/s}$ , respectively.

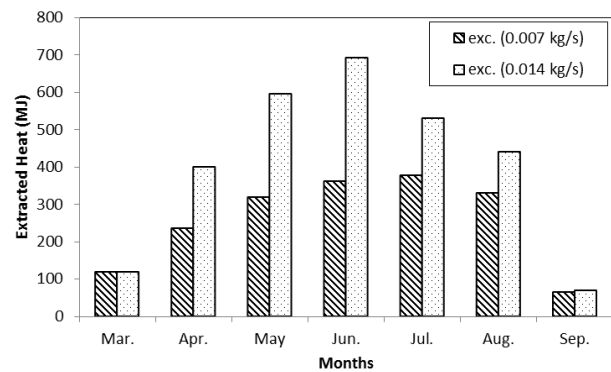


**Figure 8.** Extracted heat from the solar pond for different flow rates

Some of the solar energy reaching the surface of the solar pond is reflected by the surface of the pond. The rest of the solar radiation is transmitted to the pond and

radiation is absorbed as it passes through the layers. Solar energy, reaching the storage zone of the solar pond is stored thermally. The stored heat energy was extracted by using the heat exchanger. The heat extraction ratio (HER) is calculated by using Eq. 4. The heat extraction rate is important in that it shows how much of the incoming solar energy is extracted. Figure 9 shows the heat extraction ratio for different flow rates. The maximum and minimum heat extraction ratio (HER) is 13.39 % in July and 2.96 % in September for 0.007 kg/s; 24.27 % in June and 3.23 % in September for 0.014 kg/s, respectively. As the system started to operate in March, the heat extraction rate in March was low. The rate of heat extraction increases rapidly after the temperature of the system increases. As the heat is extracted from the solar pond, there is also the possibility of converting more of the solar energy to heat energy.

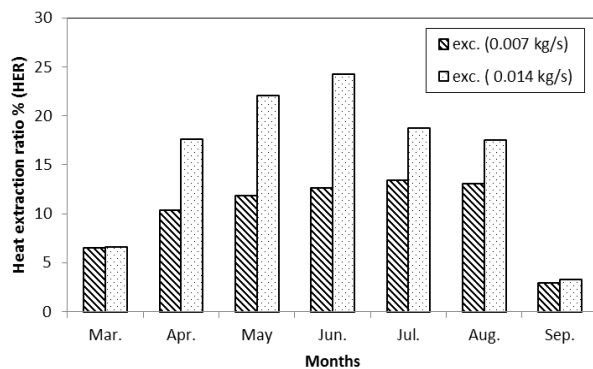


**Figure 9.** Heat extraction ratio for different flow rates

## CONCLUSION

In order to improve the efficiency of solar ponds, the heat conversion rate of solar energy reaching the surface of the pond should be increased. By extracting heat from the solar pond, more solar energy can be converted into heat energy. In this study, a numerical calculation was performed to investigate the performance of the solar pond. Furthermore, the results were compared with an experiment (solar pond 2 m × 2 m × 1.6 m in size) which was built in the university campus of Cukurova. The solar pond with the same dimensions was modeled in a computer environment and simulated with commercial software COMSOL. Daily pressure and temperature values were taken from the meteorology. ASHRAE Weather Data Viewer 5.0 was used for ambient data processing. The maximum and minimum heat extraction ratio (HER) is 13.39 % in July and 2.96 % in September for 0.007 kg/s; 24.27 % in June and 3.23 % in September for 0.014 kg/s, respectively.

In many other studies, since the heat is not taken out by integrating an exchanger into the system, the pond temperature remains constant as the pond temperature reaches stable conditions and heat lost equals heat

absorbed, depending on the solar energy coming in during the day. In this case, it is not possible to estimate exactly how much of the stored heat can actually be used. However, when the heat is extracted, the real behavior of the pond emerges. Thus, the ratio of the energy stored in the pond to the energy coming to the pond surface can be increased. It is observed that from March to the end of September, a positive heat flow is achieved and the solar pond maintains its thermal efficiency. For the other months, the system can be used for primary heating by keeping the inlet temperature low.

## ACKNOWLEDGMENT

The authors would like to thank to Adiyaman University and Middle East Technical University for technical support.

## REFERENCES

- Adana Meteorology Regional Office, 2018, *Turkish State Meteorological Service*, Ankara, Turkey.
- Alcaraz A., Valderrama C., Cortina J.L., Akbarzadeh A. and Farran A., 2016, Enhancing the efficiency of solar pond heat extraction by using both lateral and bottom heat exchangers, *Solar Energy*, 134, 82-94.
- Alcaraz A., Montalà M., Valderrama C., Cortina J.L., Akbarzadeh A. and Farran A., 2018, Increasing the storage capacity of a solar pond by using solar thermal collectors: Heat extraction and heat supply processes using in-pond heat exchangers, *Solar Energy*, 17, 112-121.
- Amirifard M., Kasaeian A. and Amidpour M., 2018, Integration of a solar pond with a latent heat storage system, *Renewable Energy*, 125, 682-693.
- Aramesh M., Pourfayaz F. and Kasaeian A., 2017, Numerical investigation of the nanofluid effects on the heat extraction process of solar ponds in the transient step, *Solar Energy*, 157, 869-879.
- Assari M.R., Tabrizi H.B. and Beik A.J.G., 2015, Experimental studies on the effect of using phase change material in salinity-gradient solar pond, *Solar Energy*, 122, 204-214.
- Bozkurt I. and Karakilcik M., 2012, The daily performance of a solar pond integrated with solar collectors, *Solar Energy*, 86, 1611-1620.
- Bozkurt I., Atiz A., Karakilcik M. and Dincer I., 2014, An investigation of the effect of transparent covers on the performance of cylindrical solar ponds, *International Journal of Green Energy*, 11, 404-416.

- Bozkurt I. and Karakilcik M., 2015, The effect of sunny area ratios on the thermal performance of solar ponds, *Energy Conversion and Management*, 91, 323–332.
- Bryant H.C. and Colbeck I., 1977, A solar pond for London, *Solar Energy*, 19, 321–322.
- COMSOL, 2018, *Heat Transfer Module*, <https://www.comsol.com> [accessed 30 December 2020]
- Date A., Yaakob Y., Date A., Krishnapillai S. and Akbarzadeh A., 2013, Heat extraction from Non-Convective and Lower Convective Zones of the solar pond: A transient study, *Solar Energy*, 97, 517–528.
- El-Sebaï A.A., Aboul-Enein S., Ramadan M.R.I. and Khallaf A.M., 2013, Thermal performance of shallow solar pond under open and closed cycle modes of heat extraction, *Solar Energy*, 95, 30–41.
- Karakilcik M., Bozkurt I. and Dincer I., 2013a, Dynamic exergetic performance assessment of an integrated solar pond, *Int. J. Exergy*, 12, 70–86.
- Karakilcik M., Dincer I., Bozkurt I. and Atiz A., 2013b, Performance assessment of a solar pond with and without shading effect, *Energy Conversion and Management*, 65, 98–107.
- Karakilcik M., Dincer I. and Rosen M.A., 2006, Performance investigation of a solar pond, *Applied Thermal Engineering*, 26, 727–735.
- Khalilian M., Pourmokhtar H. and Roshan A., 2018, Effect of heat extraction mode on the overall energy and exergy efficiencies of the solar ponds: A transient study, *Energy*, 154, 27–37.
- Leblanc J., Akbarzadeh A., Andrews J., Lu H. and Golding P., 2011, Heat extraction methods from salinity-gradient solar ponds and introduction of a novel system of heat extraction for improved efficiency, *Solar Energy*, 85, 3103–3142.
- Mansouri A.E., Hasnaoui M., Amahmid A. and Dahani Y., 2018, Transient theoretical model for the assessment of three heat exchanger designs in a large-scale salt gradient solar pond: Energy and exergy analysis, *Energy Conversion and Management*, 167, 45–62.
- Modest M.F., 2013, *Radiative Heat Transfer*, 2nd ed., San Diego, California: Academic Press.
- Renewables 2017 *Global Status Report*, 2018, <http://www.ren21.net/gsr-2017/> (accessed 19 September 2018).
- Sogukpinar H., Bozkurt I., Karakilcik M. and Cag S., 2016, Numerical evaluation of the performance increase for a solar pond with glazed and unglazed, *IEEE International Conference on Power and Renewable Energy*, 598–601, doi: 10.1109/ICPRE.2016.7871146
- Sogukpinar H., Bozkurt I. and Karakilcik M., 2018, Performance Comparison of Aboveground and Underground Solar Ponds, *Thermal Science*, 22, 953–961.